Performance Analysis of a 4-DOF Integrated Seat, Cabin and Wheel Suspension System*

[1]K. Eddah, [1]O. A. Dahunsi, [1]A. Simons and [1]S. Nunoo
[1]University of Mines and Technology (UMaT), Tarkwa Ghana

Eddah, K., Dahunsi, O., A., Simons, A. and Nunoo, S. (2020), "Performance Analysis of a 4-DOF Integrated Seat, Cabin and Wheel Suspension System", *Ghana Journal of Technology*, Vol. 5, No. 1, pp. 1 - 11.

Abstract

Contemporary research studies has treated wheel suspensions, truck cabin suspensions and seat suspension systems as separate entities whereas they are related. The dynamics of the individual systems and driver biomechanics contributes to the overall system dynamics. In this study, a combined seat, cabin and wheel suspension quarter vehicle of the 10 wheeled truck was modelled and simulated for response to deterministic and random road disturbance inputs (modelled based on ISO road class C and F for vehicle speeds of 45 km/h and 27 km/h respectively). Root-Mean-Squared (RMS) acceleration value of 1.071 m/s^2 was attained for the driver seat with the deterministic road disturbance input, while 1.172 m/s^2 and 8.661 m/s^2 were attained for the random road disturbance input at the two specified speeds respectively. The frequency domain analysis reveal that the seat mass acceleration response was amplified in the frequency band of 0.154 Hz and 8.69 Hz having a peak gain of 46.8 dB at 1.4 Hz. The frequency response also shows an amplification of vibration in the band of 0.155 Hz and 15.5 Hz attaining a maximum gain of 43.7 dB at 1.4 Hz for cabin and 0.158 Hz and 385 Hz attaining a maximum of 49 dB at 1.46 Hz for chassis. The system is stable and largely presented suspension travel values less than 11 cm but the vertical vibration values exceeded the ISO stipulated limits.

Keywords: Suspension System, Whole-Body Vibration (WBV), Bode Plot, Time Domain Analysis

1 Introduction

The mining sector plays a major role in the Ghanaian economy. This sector uses various grades of work vehicles in their day-to-day activities. Some work vehicles used include buses, crawlers, excavators, dump trucks, and motor graders (Anon., 2018).

Among these work vehicles, the 10-wheeled, 3-axle 6×4 rigid dump truck, with single point tandem bogie rear suspension, is prominent and largely used for material transportation. Fig. 1 shows a pictorial view of the common 10 wheeled, 3-axle dump truck, while Fig. 2 shows the 2-D lumped mass schematic representation of the 10-wheeled, 3-axle dump truck.

The dump truck is equipped with vehicle suspension system, which acts as low pass filter and attenuates mechanical vibrations transmitted to truck operators. Conventionally, vehicle suspension consists of an elastic element, a damping element, and suspension links (Savaresi *et al*., 2010).

Vehicle suspensions are classified into three main types, namely, Passive Vehicle Suspension (PVSS), Semi-Active Vehicle Suspension (SAVSS), and Active Vehicle Suspension (AVSS) (Dahunsi, 2013; Savaresi, *et al*., 2010; Tahir *et al*., 2014). While the demand for better comfort and demonstrated technological growth is pushing for actualisation of AVSS or SAVSS in commercial and smaller vehicles, PVSS remain relatively cheap and reliable. Except in military applications, PVSS appears to be sufficient for heavy-duty vehicles (El-Demerdash, 2002; Ibrahim *et al.*, 2003).

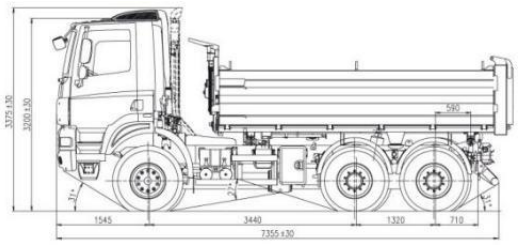

Fig. 1 Pictorial View of a 10-wheeled, Three axle Dump Truck (Source: Tatra Defence Industries limited, 2020)

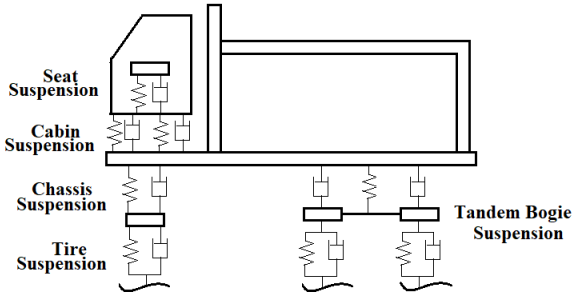

Fig. 2 Lumped Mass Schematic of the 10-Wheeled, Three Axle Truck

The rough and undulating road conditions predisposes off-road vehicles and occupants to road induced Whole-Body Vibration (WBV). Work vehicle operators are major victims of WBV exposure and from the works of Akinnuli *et al.*

*Manuscript received April 19, 2020
Revised version accepted September 22, 2020

(2018) and Mayton *et al*. (2018), work vehicle operators are exposed to unacceptable levels of WBV. Effects of WBV exposure on vehicle operators include fatigue, annoyance, drowsiness and Low Back Pains (LBPs).

Several documented studies on side effects of WBV exposure on seated occupants are available in Bovenzi (1992), Griffin (1994), and Paddan and Griffin (2002). In such studies, Griffin (1994), sampled 16 test participants who were subjected to fore-and-aft and lateral random vibration in a frequency range of 0.5 to 10 Hz whiles reading a newspaper. He reported that their reading speed significantly reduced in the frequency range of 1.25 to 6.3 Hz with the maximum reading impairment occurring at 4.0 Hz.

Conversant with work related hazards posed by WBV exposure, International Organisation for Standardisation (ISO), British Standard Institution (BSI), and American National Standard Institute (ANSI), have published recommended standards, which must be adhered to in order to minimise WBV exposure. According to Coyte *et al*. (2015), studies in WBV exposure and analysis are grouped into ergonomics, biomechanics and vehicle dynamics.

Research efforts directed at minimising WBV exposure in vehicles thereby ensuring good ride comfort exeperiences are focussed on vehicle suspension design and optimization. The main challenge in vehicle suspension design is the achievement of an optimum design with the appropriate trade-off between the conflicting suspension performance criteria like ride quality, vehicle handling, road holding and suspension travel (Dahunsi *et al*., 2020; Savaresi *et al*., 2010).

While modern day vehicle suspension design research continues in the three highlighted classes of vehicle suspensions, it has become necessary to estimate the most critical suspension design between three existing suspension levels in a truck. Most works in the literature choose to either focus on seat suspension, cabin suspension or wheel suspension design.

The first group of research works, which focussed on wheel suspension design include Dahunsi (2020); Kaleemullah *et al. (*2019); Shafie *et al.* (2015); and Song *et al.* (2017). The second group focussed on seat suspension design, and include Alfadhli *et al. (*2018); Dahunsi (2016); and Gohari and Tahmasebi (2015); and Ning *et al. (*2016). These works demonstrated that good seat suspension design achieve good ride comfort in the frequency range of 2 – 6 Hz. The third group which focussed on cabin suspension design include Ekberg and Hansson (2015); Graf *et al.* (2009); and Sim *et al*. (2017). In this work, these three levels of suspensions are integrated in a four degree of freedom (4-DOF) lumped parameter model of a quarter vehicle model such that the overall and individual suspension performances could be studied.

Maciejewski (2012), Gudarzi and Oveisi (2014) and Yao *et al*. (2013) coupled the driver biomechanics with seat dynamics in order to analyse the combined case as a unit. However, the issue of WBV exposure and the transmissibility of mechanical vibrations to seated occupants is one that needs to be treated as a combined case, incorporating vehicle suspension, seat suspension, driver biomechanics and in the case of trucks, cabin suspension. This is because the dynamics of the vehicle frame, cabin, seat, and wheel affects the levels of WBV exposure to vehicle operators.

In line with this view, Du *et al*. (2012), and Kuznetsov *et al*. (2011) have recommended and studied the combined vehicle model to ascertain the levels of discomfort to seated occupants. There has been a number of such studies on integrated suspension design. However, most of these are for luxury vehicles and commuter vehicles. The purpose of this paper is to model and simulate the dynamic behaviour of a linear quarter truck suspension for vibration analysis in the time and frequency domain taking into consideration the combined case of wheel, seat, and cabin and to ascertain the stability of the modelled system.

2 Resources and Methods Used

2.1 Linear Quarter Truck Modelling

Consider the 4-DOF lumped parameter quarter vehicle model of the 10-wheel truck incorporating the seat, cabin and wheel suspension of the vehicle shown in Fig. 3.

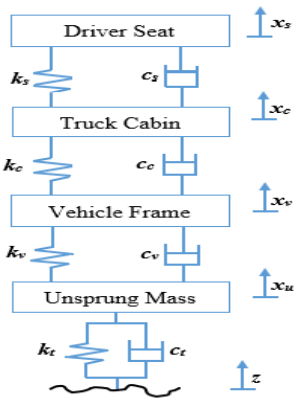

Fig. 3 Quarter Truck Model

The masses, m_u, m_v, m_c and m_s are the unsprung mass or mass of the wheel unit, mass of the chassis, mass of the cabin and mass of the seat unit. Similar representation goes for the spring stiffnesses, k_u, k_v,

k_c and k_s and damping coefficients c_u, c_v, c_c and c_s respectively. The vertical displacement for the wheel, chassis, cabin and the seat suspensions are given by x_u, x_v, x_c and x_s. The system is excited by a road disturbance input, z.

2.2 Mathematical Modelling

The system equations are given by equations 1-4. The nonlinear components of the elements are neglected for the purpose of simplicity. The dynamic equation for driver seat motion is given as:

$$m_s\ddot{x}_s = -k_s(x_s - x_c) - c_s(\dot{x}_s - \dot{x}_c)$$

$$\ddot{x}_s = \frac{1}{m_s}\left[-k_s(x_s - x_c) - c_s(\dot{x}_s - \dot{x}_c)\right] \quad (1)$$

The dynamic equation for the cabin motion is given as:

$$m_c\ddot{x}_c = k_s(x_s - x_c) + c_s(\dot{x}_s - \dot{x}_c) - k_c(x_c - x_v) - c_c(\dot{x}_c - \dot{x}_v)$$

$$\ddot{x}_c = \frac{k_s}{m_c}x_s - \left(\frac{k_s}{m_c} + \frac{k_c}{m_c}\right)x_c + \frac{k_c}{m_c}x_v + \frac{c_s}{m_c}\dot{x}_s - \left(\frac{c_s}{m_c} + \frac{c_c}{m_c}\right)\dot{x}_c + \frac{c_c}{m_c}\dot{x}_v \quad (2)$$

The dynamic equation for the vehicle frame motion is given as:

$$m_v\ddot{x}_v = k_c(x_c - x_v) + c_c(\dot{x}_c - \dot{x}_v) - k_v(x_v - x_u) - c_v(\dot{x}_v - \dot{x}_u)$$

$$\ddot{x}_v = \frac{k_v}{m_v}x_c - \left(\frac{k_c}{m_v} + \frac{k_v}{m_v}\right)x_v + \frac{k_v}{m_v}x_u + \frac{c_c}{m_v}\dot{x}_c - \left(\frac{c_c}{m_v} + \frac{c_v}{m_v}\right)\dot{x}_v + \frac{c_v}{m_v}\dot{x}_u \quad (3)$$

The dynamic equation for the unsprung mass motion is given as:

$$m_u\ddot{x}_u = k_v(x_v - x_u) + c_v(\dot{x}_v - \dot{x}_u) + k_t(z - x_u) + c_t(\dot{z} - \dot{x}_u)$$

$$\ddot{x}_u = \frac{k_v}{m_u}x_v - \left(\frac{k_v}{m_u} + \frac{k_t}{m_u}\right)x_u + \frac{k_t}{m_u}z + \frac{c_v}{m_u}\dot{x}_v - \left(\frac{c_v}{m_u} + \frac{c_t}{m_u}\right)\dot{x}_u + \frac{c_t}{m_u}\dot{z} \quad (4)$$

2.2.1 State-Space Representation

The state-space representation of a continuous-time linear dynamical system can be written in the form of Equation 5 and 6.

$$\dot{x} = A(t)x(t) + B(t)u(t) \quad (5)$$

$$y = C(t)x(t) + D(t)u(t) \quad (6)$$

feedforward matrix. *x(t)* is the state vector, and *u(t)* is the vector of control input. Let the state variables be $x_1 = x_s$, $x_2 = x_c$, $x_3 = x_v$, $x_4 = x_u$, $x_5 = z$, $x_6 = \dot{x}_s$, $x_7 = \dot{x}_c$, $x_8 = \dot{x}_v$, $x_9 = \dot{x}_u$, and $x_{10} = \dot{z}$. thus , the vector of state variable is given as: $x = [x_1 \quad x_2 \quad x_3 \quad x_4 \quad x_5 \quad x_6 \quad x_7 \quad x_8 \quad x_9 \quad x_{10}]^T$ and the state space model is given by equation 6 and 7.

2.3 Road Disturbance Input

Two types of road disturbance input is chosen for this study, a deterministic road disturbance input, and random road disturbance input. These models are discussed in the following sub-sections.

2.3.1 Deterministic Road Disturbance Input

The deterministic road disturbance input used for the analysis consists of a sinusoidal hump (6.7 cm high) (Dahunsi, 2013), and a smooth pothole with height 5 cm (high severity level pothole) (Cao *et al.*, 2011). The hump and pothole can be modelled using equation 1 (Dahunsi, 2013).

$$Z(t) = \begin{cases} \frac{a_1}{2}\left(1 - \cos\frac{2\pi vt}{\lambda}\right) & 1 \le t \le 1.25 \\ -\frac{a_2}{2}\left(1 - \cos\frac{2\pi vt}{\lambda}\right) & 6 \le t \le 6.25 \\ 0 & \text{Otherwise} \end{cases} \quad (7)$$

where v is velocity of truck (27 km/h), a_1 is amplitude of the hump, a_2 is amplitude of pothole, and λ is half the wavelength of a sinusoidal road undulation, which is 4 m. The MATLAB plot for the deterministic road disturbance input is shown in Fig. 4.

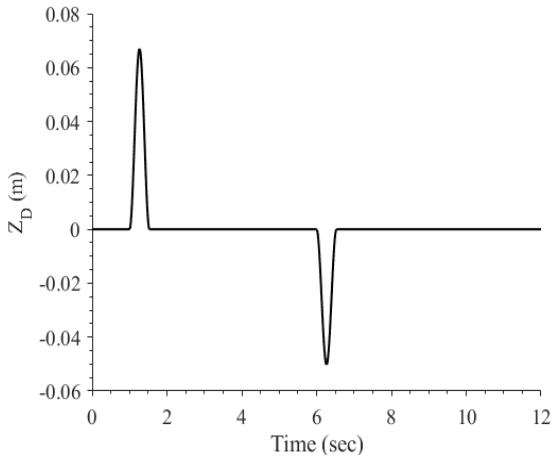

Fig. 4 Deterministic Road Disturbance Input

2.3.2 Random Road Disturbance Input

ISO 8608 (2016) classifies roads according to their degree of roughness as shown in Table 1. The random road employed for this study belongs to road class C with a geometric mean spatial frequency of 0.000256 m^3 and road class F with a geometric mean spatial frequency of 0.016384 m^3. This is modelled based on equation 8. The random road disturbance input can be modelled using equation 8 (Dahunsi, 2013).

$$\dot{z}_R = 2\pi n_0 z_R + \sqrt{G_0 V} W_0(t) \qquad (8)$$

where $W_0(t)$ is a zero variance white Gaussian noise, $\dot{z}_R$ is the vertical wheel velocity, z_R is the vertical wheel displacement, V is the forward velocity of vehicle, n_0 is the reference spatial frequency and G_0 is the road roughness coefficient. The plot for random road disturbance input (based on ISO road class C) is shown in Fig. 5 and that for the random road disturbance input based on ISO road class F is shown Fig. 6.

Table 1 ISO Road Classification

Road class	Degree of Roughness		
	Lower limit	Geometric mean	Upper limit
	Spatial frequency units, n $G_d(n_0)^a$ 10^{-6} m^3		
A	—	16	32
B	32	64	128
C	128	256	512
D	512	1 024	2 048
E	2 048	4 094	8 192
F	8 192	16 384	32 768
G	32 768	65 536	131 072
H	131 072	262 144	—

(Source: ISO 8608, 2016)

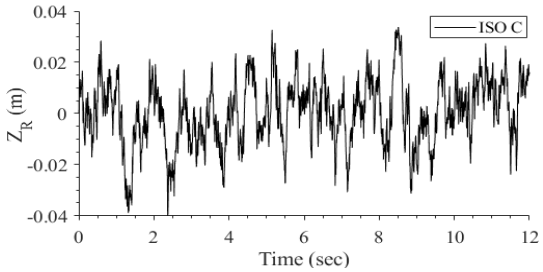

Fig. 5 Random Road Disturbance Input based on ISO Road Class C

The random road intensity for ISO road class C as modelled in Fig. 5 as the vehicle moves at a speed of 45 km/h, ranges between a minimum value of -4.013 cm, occurring at 2.367 sec, and a maximum of +3.381 cm occurring at 8.507 sec.

For ISO road class F, the random road intensity for this class, at a vehicle speed of 27 km/h, ranges between a minimum value of -30.07 cm, occurring at 1.407 sec, and a maximum of +25.88 cm, occurring at 8.587 sec shown in Fig. 6.

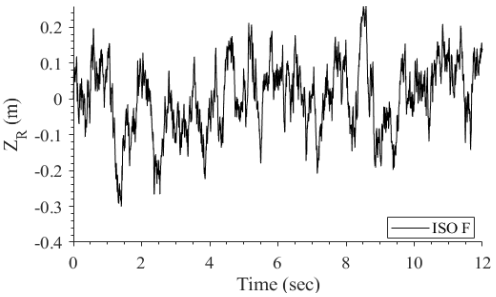

Fig. 6 Random Road Disturbance Input based on ISO Road Class F

$$\begin{bmatrix} \dot{x}_1 \\ \dot{x}_2 \\ \dot{x}_3 \\ \dot{x}_4 \\ \dot{x}_5 \\ \dot{x}_6 \\ \dot{x}_7 \\ \dot{x}_8 \\ \dot{x}_9 \\ \dot{x}_{10} \end{bmatrix} = \begin{bmatrix} 0 & 0 & 0 & 0 & 0 & 1 & 0 & 0 & 0 & 0 \\ 0 & 0 & 0 & 0 & 0 & 0 & 1 & 0 & 0 & 0 \\ 0 & 0 & 0 & 0 & 0 & 0 & 0 & 1 & 0 & 0 \\ 0 & 0 & 0 & 0 & 0 & 0 & 0 & 0 & 1 & 0 \\ 0 & 0 & 0 & 0 & 0 & 0 & 0 & 0 & 0 & 1 \\ -\frac{k_s}{m_s} & \frac{k_s}{m_s} & 0 & 0 & 0 & -\frac{c_s}{m_s} & \frac{c_s}{m_s} & 0 & 0 & 0 \\ \frac{k_s}{m_c} & -\left(\frac{k_c+k_v}{m_c}\right) & \frac{k_c}{m_c} & 0 & 0 & \frac{c_s}{m_c} & -\left(\frac{c_s+c_c}{m_c}\right) & \frac{c_c}{m_c} & 0 & 0 \\ 0 & \frac{k_c}{m_v} & -\left(\frac{k_c+k_v}{m_v}\right) & \frac{k_v}{m_v} & 0 & 0 & \frac{c_c}{m_v} & -\left(\frac{c_c+c_v}{m_v}\right) & \frac{c_v}{m_v} & 0 \\ 0 & 0 & \frac{k_v}{m_u} & -\left(\frac{k_v+k_t}{m_u}\right) & \frac{k_t}{m_u} & 0 & 0 & \frac{c_v}{m_u} & -\left(\frac{c_v+c_t}{m_u}\right) & \frac{c_t}{m_u} \\ 0 & 0 & 0 & 0 & 0 & 0 & 0 & 0 & 0 & 1 \end{bmatrix} \begin{bmatrix} x_1 \\ x_2 \\ x_3 \\ x_4 \\ x_5 \\ x_6 \\ x_7 \\ x_8 \\ x_9 \\ x_{10} \end{bmatrix} + [0]u(t) \qquad \text{.... (6)}$$

$$[y] = \begin{bmatrix} -\frac{k_s}{m_s} & \frac{k_s}{m_s} & 0 & 0 & 0 & -\frac{c_s}{m_s} & \frac{c_s}{m_s} & 0 & 0 & 0 \end{bmatrix} \begin{bmatrix} x_1 \\ \vdots \\ \vdots \\ x_{10} \end{bmatrix} + [0]u(t) \qquad (7)$$

3 Results and Discussion

3.1 Simulation and Analysis

The governing equations 1 to 4 were built into MATLAB Simulink model, to study and observe the dynamic response of the system over a period of 12 s using physical parameters in Table 2.

Table 2 Truck Parameter Specification

Parameter	Value	Parameter	Value
m_s (kg)	120	m_v (kg)	3800
k_s (N/m)	29000	k_v (N/m)	500000
c_s (Ns/m)	900	c_v (Ns/m)	11000
m_c (kg)	1250	m_u (kg)	775
k_c (N/m)	34000	k_t (N/m)	647000
c_c (Ns/m)	3760	c_t (Ns/m)	250

(Source: Abdelkareem et al., 2018)

3.2 Time Domain Response

The Root-Mean-Squared (RMS) acceleration (expressed in equation 9), is often abbreviated as $A_{RMS,}$ is the approach endorsed by the ISO (ISO 2631-1, (1997); Akinnuli *et al.*, 2018). The RMS acceleration is defined as:

$$A_{RMS} = \sqrt[2]{\frac{1}{T}\int_0^T a_w{}^2(t)dt} \tag{9}$$

where T is the overall period of exposure in seconds, and $a_w(t)$ is the acceleration at time t in m/s^2. Table 3 presents the ISO scale for discomfort in vehicles.

Table 3 International Standards Scale of Discomfort

Intervals of frequency-weighted vertical acceleration (m/s^2)	Comfort Levels
< 0.315	not uncomfortable
0.315 to 0.63	a little uncomfortable
0.5 to 1	fairly uncomfortable
0.8 to 1.6	uncomfortable
1.25 to 2.5	very uncomfortable
> 2	extremely uncomfortable

(Source: ISO 2631, 2003)

The Transmissibility of Acceleration (ToA) and Transmissibility of Displacement (ToD) values (equation 10 and 11) indicates how much acceleration and displacement is transmitted from the truck cabin to the driver seat.

$$ToA = \frac{Seat\ A_{RMS}}{Cabin\ A_{RMS}} \tag{10}$$

$$ToD = \frac{Seat\ X_{RMS}}{Cabin\ X_{RMS}} \tag{11}$$

3.2.1 System Response to Deterministic Road Disturbance Input

Simulations carried out in the time domain, considering a vehicle speed of 27 km/h for the deterministic road disturbance input shows that vertical A_{RMS} values of 1.071 m/s^2, 0.7939 m/s^2 and 1.253 m/s^2, respectively, were obtained for vehicle seat, cabin and chassis. These values represent 36.64% attenuation in mechanical vibration from the vehicle chassis to cabin, and an amplification of 34.90% for vibration signal moving from cabin to driver seat. The passive quarter truck model (for the deterministic road disturbance input) achieves an overall attenuation of 14.53% in mechanical vibration from the chassis to the driver seat. These results can be observed from Fig. 7, which shows the vertical accelerations for the driver seat, truck cabin and vehicle frame or chassis.

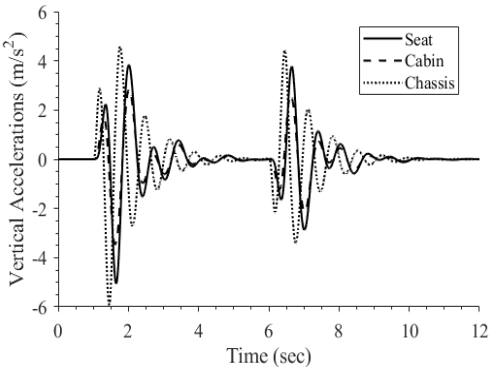

Fig. 7 System Acceleration Response to Deterministic Road Disturbance Input for Vehicle Speed of 27 km/h

The vertical A_{RMS} value for seat was found to be greater than that of the cabin and above the ISO specified upper limit of 0.93 m/s^2 similarly, the vertical A_{RMS} value for the cabin was found to be above the stipulated ISO lower bound value of 0.47 m/s^2 stipulated by the (ISO 2631-1, 1997).

From the vertical A_{RMS} values, a 1.349 ToA can be observed from time domain simulations for vehicle speed of 27 km/h for the deterministic road disturbance input. These values indicate that the seat suspension system is ineffective for vibration attenuation in the vertical direction.

The root-mean-squared displacement (X_{RMS}) values of 0.02486 m (being the greatest was recorded for the driver seat mass), 0.02167 m for the truck cabin

and 0.01897 m (being the smallest was observed for the vehicle frame). These values represent a 1.1472 Transmissibility of Displacement (ToD) for the system's response to deterministic road disturbance input for vehicle speed of 27 km/h as shown in Fig. 8.

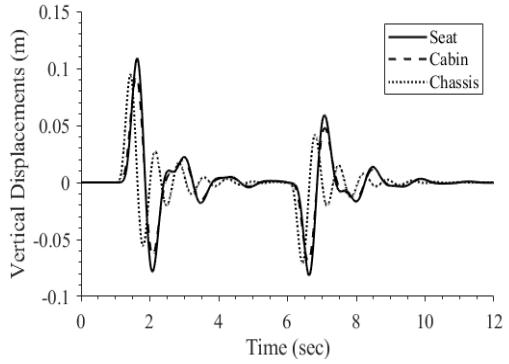

Fig. 8 System Displacement Response to Deterministic Road Disturbance Input for Vehicle Speeds of 27 km/h

The seat suspension travel was smallest having a value of ±1.774 cm, that for the wheel suspension travel was ±3.9875 cm and that for the cabin (being the greatest) was ±9.925 cm for the deterministic road disturbance input for vehicle speed of 27 km/h as shown in Fig. 9.

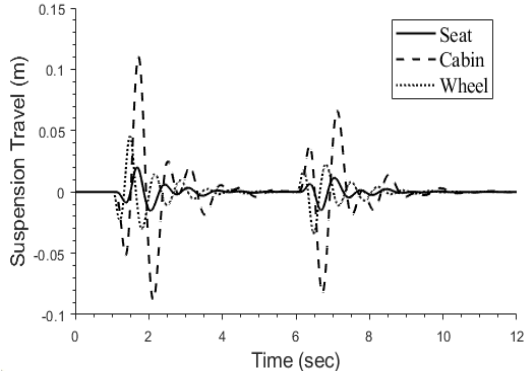

Fig. 9 Truck Suspension Travel for Vehicle Speed of 27 km/h

3.2.2 System Response to Random Road Disturbance Input Modelled based on ISO Road Class F for Vehicle Speed of 27 km/h

Simulations carried out in the time domain, considering a vehicle speed of 27 km/h for the random road disturbance input (based on ISO road class F) shows that vertical A_{RMS} values of 8.661 m/s^2, 6.258 m/s^2 and 12.26 m/s^2, respectively, were obtained for driver seat, truck cabin and vehicle frame. These values represent 48.96% attenuation in mechanical vibration from the vehicle chassis to cabin, and an amplification of 38.40% for vibration signal moving from cabin to driver seat.

The passive quarter truck model, for the random road disturbance input based on ISO road class F, achieved an overall attenuation of 29.36% in mechanical vibration from the chassis to the driver seat. These results can be observed from the Fig. 10 which showed the vertical accelerations for the driver seat, truck cabin and vehicle frame or chassis for vehicle speed of 27 km/h using ISO road class F.

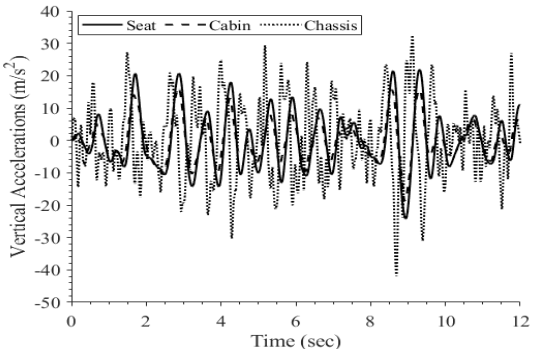

Fig. 10 System Acceleration Response to Random Road Disturbance (ISO Road Class F) for Vehicle Speed of 27 km/h

The vertical A_{RMS} value for driver seat, truck cabin and vehicle frame were found to be far above the upper limit of 0.93 m/s^2 stipulated by ISO 2631-1, (1997). From the vertical A_{RMS} values, a 1.384 ToA can be observed from time domain simulations for vehicle speed of 27 km/h for the random road disturbance input modelled based on ISO road class F. These values also indicate that the seat suspension system is ineffective for vibration attenuation in the vertical direction for the random road disturbance input.

The RMS displacement (X_{RMS}) values of 0.1897 m (being the greatest was recorded for the driver seat mass), 0.1644 m for the truck cabin and 0.1460 m being the smallest was observed for the vehicle frame. These values represent a 1.154 ToD for the system's response to random road disturbance input (based on ISO road class F) for vehicle speed of 27 km/h as shown in Fig. 11.

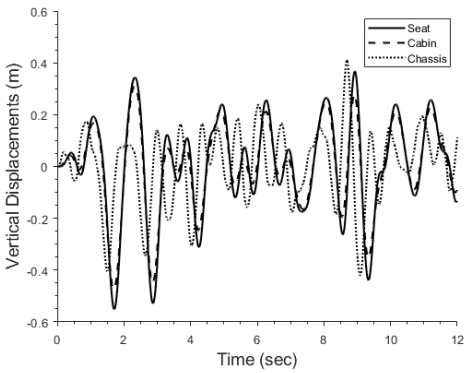

Fig. 11 System Displacement Response to Random Road Disturbance (ISO Road Class F) for Vehicle Speed of 27 km/h

The seat suspension travel was smallest having a value of ±9.245 cm, that for the wheel suspension travel was ±25.215 cm, and that for the cabin (being the greatest) was ±53.05 cm for the random road disturbance input for vehicle speed of 27 km/h as shown in Fig. 12.

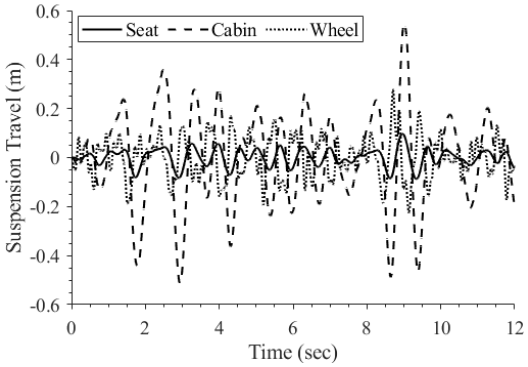

Fig. 12 Truck Suspension Travel for Vehicle Speed of 27 km/h (based on ISO Road Class F)

3.2.3 System Response to Random Road Disturbance Input Modelled based on ISO Road Class C for Vehicle Speed of 45 km/h

Simulations carried out in the time domain, considering a vehicle speed of 45 km/h for the random road disturbance input (based on ISO road class C) shows that vertical A_{RMS} values of 1.172 m/s^2, 0.8291 m/s^2 and 1.7720 m/s^2, respectively, were obtained for driver seat, truck cabin and vehicle frame. These values represent 53.21% attenuation in mechanical vibration from the vehicle chassis to cabin, and an amplification of 41.36% for vibration signal moving from cabin to driver seat.

The passive quarter truck model (for the random road disturbance input based on ISO road class C) achieves an overall attenuation of 33.86% in mechanical vibration from the chassis to the driver seat. These results can be observed from Fig. 13, which shows the vertical accelerations for the driver seat, truck cabin and vehicle frame or chassis for vehicle speed of 45 km/h using ISO road class C.

The vertical A_{RMS} value for driver seat and vehicle frame were found to be above the upper Limit Value of 0.93 m/s^2 and that of the cabin was to be within the Health Guidance and Caution Zone (HGCZ) (i.e. between 0.47 m/s^2 and 0.93 m/s^2) stipulated by the ISO 2631-1. From the vertical A_{RMS} values, a 1.414 ToA can be observed from time domain simulations for vehicle speed of 45 km/h for the random road disturbance input modelled based on ISO road class C. These values also indicate that the seat suspension system is ineffective for vibration attenuation in the vertical direction for the random road disturbance input under consideration.

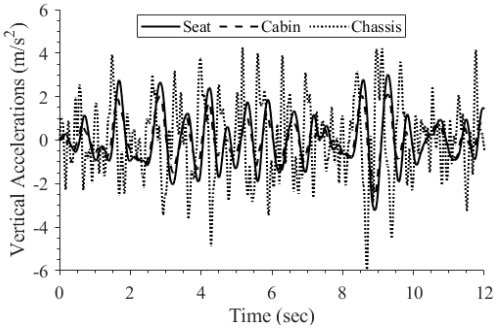

Fig. 13 System Acceleration Response to Random Road Disturbance (ISO Road Class C) for Vehicle Speed of 45 km/h

The RMS displacement (X_{RMS}) values of 0.02313 m (being the greatest was recorded for the driver seat mass), 0.01969 m for the truck cabin and 0.01878 m (being the smallest was observed for the vehicle frame). These values represent a 1.175 ToD for the system's response to random road disturbance input (based on ISO road class C) for vehicle speed of 45 km/h as shown in Fig. 14.

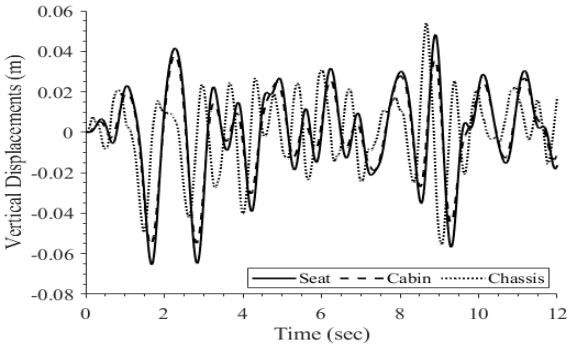

Fig. 14 System Displacement Response to Random Road Disturbance (ISO Road Class C) for Vehicle Speed of 45 km/h

The seat suspension travel was smallest having a value of ±1.254 cm, that for the wheel suspension travel was ±3.589 cm and that for the cabin (being the greatest) was ±7.01 cm for the random road disturbance input for vehicle speed of 45 km/h as shown in Fig. 15.

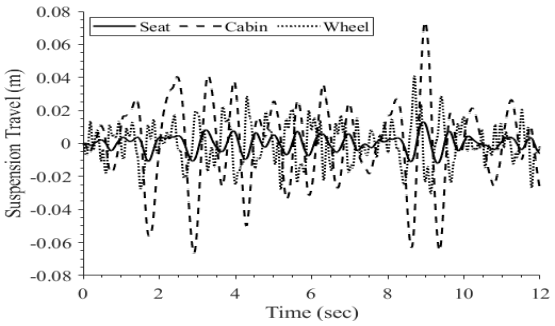

Fig. 15 Truck Suspension Travel for Vehicle Speed of 45 km/h (based on ISO Road Class C)

Using the mean spatial frequency values for the road classes given by ISO 8608 (2016), the A_{RMS} values for the linear quarter truck seat, cabin and chassis are summarised in Fig. 16 for vehicle speed of 27 km/h and in Fig. 17 for vehicle speed of 45 km/h.

It can be observed from Fig. 16 that for vehicle speed of 27 km/h, vertical A_{RMS} values (0.2712 m/s^2 for seat and 0.196 m/s^2 for cabin) for ISO road class A and cabin A_{RMS} of 0.3918 m/s^2 for ISO road class B falls below the lower bound of 0.47 m/s^2 stated by ISO 2631-1, 1997.

Also, it can be observed that, the driver seat vertical A_{RMS} value of 0.5422 m/s^2 for ISO road class B and cabin A_{RMS} of 0.7836 m/s^2 for ISO road class C fall within the Health Guidance and Caution Zone (HGCZ) (i.e. 0.47 m/s^2 < A_{RMS} < 0.93 m/s^2 whilst the remaining A_{RMS} values for the PVSS from road class C to H are above the upper bound. This shows the PVSS performance on these class of roads is unsatisfactory and requires that an AVSS be designed to reduce the A_{RMS} values to at worst within the HGCZ.

For all road classes, it can be observed that the vertical A_{RMS} value of the chassis was greatest, with the seat A_{RMS} values being intermediate and the cabin values being the least. The PVSS at this speed (27 km/h) achieves an overall average attenuation of 29.37% for all classes of road.

Likewise, from Fig. 17, for vehicle speed of 45 km/h, seat A_{RMS} values of 0.2931 m/s^2 (for ISO road class A) and cabin A_{RMS} values of 0.2073 m/s^2 (for ISO road class A) and 0.4146 m/s^2 (for ISO road class B) were found to be lower than the lower bound whilst A_{RMS} of 0.5861 m/s^2 for seat and 0.8291 m/s^2 for cabin (for ISO road class B and class C respectively) were within the HGCZ. Similar trend for vertical A_{RMS} (for V = 45 km/h) were observed for seat, cabin and chassis with an overall average attenuation of 33.86% in vibrations generated at the chassis due to the random road disturbance input as shown in Fig. 17.

3.3 Frequency Domain Analysis

Frequency domain analysis of the system based on vertical acceleration responses are presented by phase-magnitude and pole-zero map plots in Figs. 18 and 19.

The plot for seat mass acceleration shows that there exists two gain crossover frequencies of 0.154 Hz and 8.69 Hz at which a phase shift of -0.281° and -123°, respectively, will cause the close system to be unstable. The pole-zero map showed that all of the several poles are on the left hand side of the map, implying a state of stability in the system.

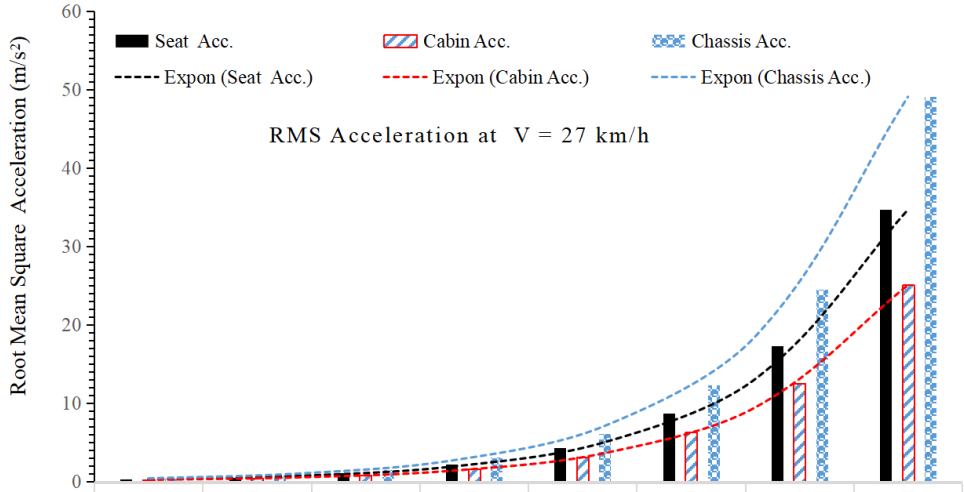

	A	B	C	D	E	F	G	H
Seat Acc.	0.2712	0.5422	1.084	2.168	4.335	8.661	17.34	34.68
Cabin Acc.	0.196	0.3918	0.7836	1.567	3.133	6.258	12.53	25.06
Chassis Acc.	0.3839	0.7677	1.535	3.07	6.138	12.26	24.55	49.1

Road Class

Fig. 16 RMS Acceleration Values for Road Class A – H at V = 27 km/h

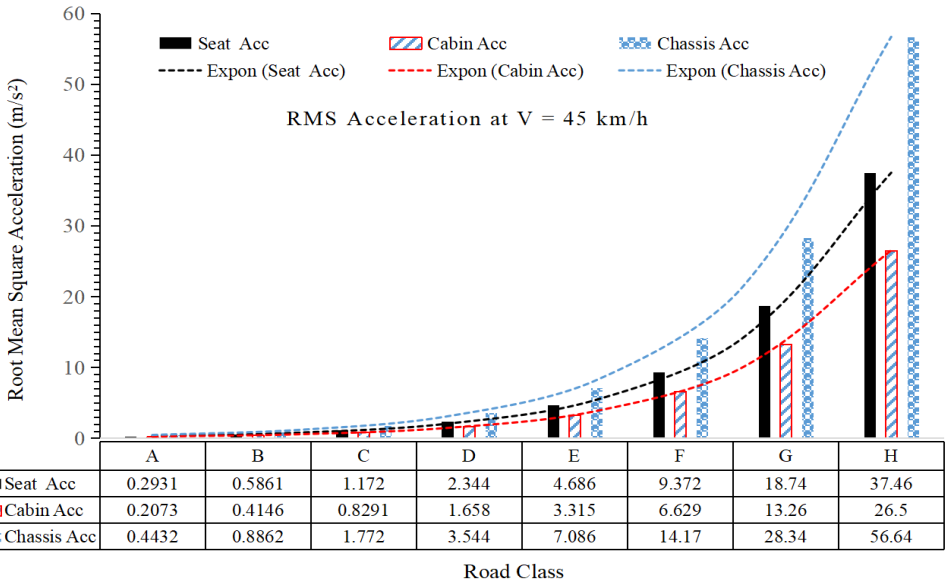

	A	B	C	D	E	F	G	H
Seat Acc	0.2931	0.5861	1.172	2.344	4.686	9.372	18.74	37.46
Cabin Acc	0.2073	0.4146	0.8291	1.658	3.315	6.629	13.26	26.5
Chassis Acc	0.4432	0.8862	1.772	3.544	7.086	14.17	28.34	56.64

Fig. 17 RMS Acceleration Values for Road Class A – H at V = 45 km/h

The passive driver seat suspension amplifies mechanical vibrations between this frequency band, attaining a maximum of 46.8 dB at 1.4 Hz and attenuates vibrations outside this frequency band. Likewise, at the phase crossover frequency of 2.99 Hz, designing a closed loop system with a gain of -31.2 dB will also result in system instability.

The plot for the cabin acceleration shows that there exists two gain crossover frequencies of 0.155 Hz and 15.5 Hz at which a phase shift of -0.276° and -15.5°, respectively, will cause system instability. The passive cabin system amplifies mechanical vibrations between these frequency bands attaining a maximum at 43.7 dB at 1.4 Hz and attenuates vibrations outside this frequency band.

This shows that the system is close to being unstable and thus the need to augment the system with an actuator and controller to ensure better the system stability. Likewise, at the phase crossover frequency of 7.54 Hz, the closed loop system with a gain of -20.1 dB will result in system instability.

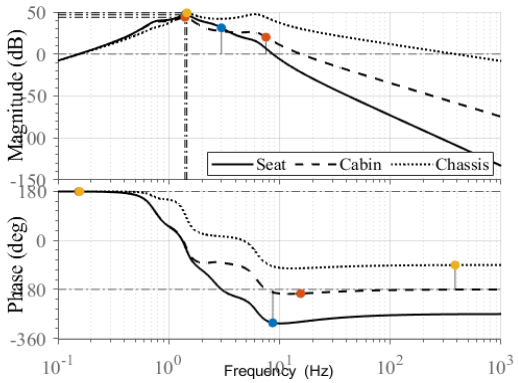

Fig. 18 Frequency Domain Analysis based on the Acceleration Responsess at the Seat, Cabin and Chassis

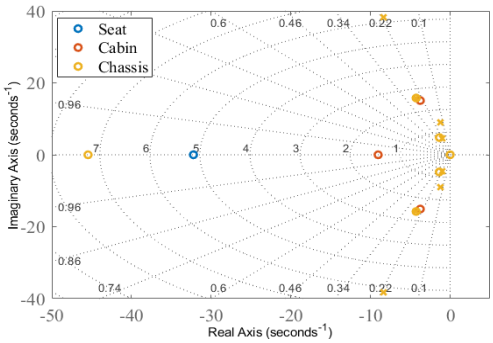

Fig. 19 Pole-Zero Map based on Acceleration Responses at the Seat, Cabin and Chassis

The bode plot for chassis mass acceleration shows that there exists two gain crossover frequencies of 0.158 Hz and 385 Hz at which a phase shift of -0.0364° and 89.4°, respectively, will cause system instability. The chassis mass amplifies input vibration between these frequency bands attaining a maximum of 49 dB at 1.46 Hz and attenuates vibration beyond this frequency band.

4 Conclusions and Recommendations

The PVSS of the quarter truck model was generally stable. Typical values of A_{RMS} recorded for the deterministic road disturbance input were 1.071 m/s^2, 0.7939 m/s^2 and 1.253 m/s^2 for seat, cabin and vehicle frame, respectively. Clearly, the seat A_{RMS} is greater that the ISO specified upperbound of 0.93 m/s^2 and that of the cabin is greater the ISO specified lower bound of 0.47 m/s^2. Results from the random road disturbance input also showed that apart from the truck cabin's A_{RMS} of 0.8291 m/s^2 for vehicle speeds of 45 km/h (for ISO road class C), A_{RMS} values for seat and cabin (based on ISO road class F) were found to be above the ISO upper

bound value of 0.93 m/s^2 stipulated by ISO 2631-1, (1997).

The frequency domain analysis showed that the seat suspension system will amplify vibration signal in the band of 0.154 – 8.69 Hz for which a phase shift of -0.281° and -123° respectively will cause seat suspension system to go unstable. Also, the cabin amplifies input vibration signal in the band of 0.155 – 15.5 Hz for which shifts of -0.276° and -15.5 Hz respectively will cause truck cabin suspension system to go unstable.

These results also showed that the peak acceleration values attained by all the suspension systems exceeded the acceptable levels stipulated by ISO 2631-1, (1997), thereby defining a need for a better performing suspension system than the existing one. In future, it will be appropriate to analyse the responses of the suspension systems with due consideration for the various nonlinear characteristics of the system. Afterwards, the design of a better performing controlled suspension system is necessary to properly attenuate the vibration signals reaching the vehicle occupants.

References

Abdelkareem, M. A., Makrahy, M. M., Abd-El-Tawwab, A. M., EL-Razaz, A. S. A., Kamal Ahmed Ali, M. and Moheyeldein, M. M., (2018), "An Analytical Study of the PerformanceIndices of Articulated Truck Semi-Trailer during Three Different Cases to Improve the Driver Comfort", *Proceedings of the Institution of Mechanical Engineers, Part K: Journal of Multi-body Dynamics*, Vol. *232, No.* 1, pp. 84-102.

Akinnuli, B. O., Dahunsi, O. A., Ayodeji, S. P. and Bodunde, O. P. (2018), "Whole-Body Vibration Exposure on Earthmoving Equipment Operators in Construction Industry," *Cogent Engineering*, pp. 1 – 14.

Alfadhli, A., Darling, J. and Hillis, A. J. (2018), "The Control of an Active Seat Suspension Using an Optimised Fuzzy Logic Controller, Based on Preview Information from a Full Vehicle Model", *Vibration*, Vol. 1, No. 1, pp. 20-40.

Anon. (2018), "Report on the Performance of the Mining Industry in 2017", *Ghana Chamber of Mines*. 41pp.

Anon. (2020), 6×6 Three-way tipper T158, retrieved from *http://tatradefenceindustrial-.com/tatra-vehicles/tatra-for-construction/6x6-three-way-tipper-t158/*. Accessed: September 3rd, 2020.

Bovenzi, M. and Zadini, A. (1992), "Self-Reported Low Back Symptoms in Urban Bus Drivers Exposed to Whole-Body Vibration", *Spine*, Vol. 17, No. 9, pp.1048-1059.

Cao, D., Song, X. and Ahmadian, M. (2011), "Editors' perspectives: Road Vehicle Suspension Design, Dynamics, and Control", *Vehicle System Dynamics*, Vol. 49, No. 1-2, pp.3-28.

Coyte, J. L., Stirling, D., Du, H. and Ros, M. (2015), "Seated Whole-Body Vibration Analysis, Technologies, and Modelling: a Survey", *IEEE Transactions on Systems, Man, and Cybernetics: Systems*, Vol. 46, No. 6, pp. 725-739.

Dahunsi, O. A. (2013), "Neural Network-based Controller Design for Active Vehicle Suspension Systems", *Unpublished PhD Thesis*, University of Witwatersrand, Johannesburg, 193pp.

Dahunsi O. A. (2016)**,** "Static and Dynamic Characteristics of Scissors-Type Guiding Mechanism Work Suspension Seat*". Journal of Machinery Manufacturing and Automation*. Vol. 5, No. 1, pp. 8-14 .

Dahunsi, O. A., Dangor, M., Pedro, J. O. and Ali, M. M. (2020), "Proportional + Integral + Derivative Control of Nonlinear Full-Car Electrohydraulic Suspensions Using Global and Evolutionary Optimization Techniques", *Journal of Low Frequency Noise, Vibration and Active Control*, Vol. 39, No. 2, pp. 393-415.

Du, H., Li, W. and Zhang, N. (2012), "Integrated Seat and Suspension Control for a Quarter Car with Driver Model", *IEEE Transactions on Vehicular Technology*, Vol. 61, No. 9, pp. 3893-3908.

El-Demerdash, S. M. (2002),"Improvement of Trucks Ride Dynamics Using a Hydraulic Semi-Active Suspension System", *SAE Transactions: Journal of Commercial Vehicles*, Vol. 111, Section 2. pp. 555-566.

Ekberg, C. and Hansson, E. (2015), "Design and Simulation of Active and Semi-Active Cab Suspensions with Focus to Improve Ride Comfort of a Heavy Truck", *Unpublished Masters' Thesis*, Chalmers University of Technology, Gothenburg, 57pp.

Gohari, M. and Tahmasebi, M. (2015), "Active Off-Road Seat Suspension System Using Intelligent Active Force Control", *Journal of Low Frequency Noise, Vibration and Active Control*, Vol. 34, No. 4, pp. 475-489.

Graf, C., Maas, J. and Pflug, H. C. (2009), "Concept for an Active Cabin Suspension", *2009 IEEE International Conference on Mechatronics*, pp. 1-6.

Griffin, M. J. and Hayward, R. A. (1994) "Effects of Horizontal Whole-Body Vibration on Reading", *Applied Ergonomics*, Vol. 25, No. 3, pp. 165-169.

Gudarzi, M. and Oveisi, A. (2014), "Robust Control for Ride Comfort Improvement of an Active Suspension System Considering Uncertain Driver's Biodynamics", *Journal of*

Low Frequency Noise, Vibration and Active Control, Vol. 33, No. 3, pp. 317-339.

International Organization for Standardization. (2016), *Mechanical Vibration and Shock-Evaluation of Human Exposure to Whole-Body Vibration-Part 1: General Requir-ements*, ISO Geneva, Switzerland (ISO Standard No. ISO 2631-1:1997/Amd. 1:2010(E)).

International Organization for Standardization. (2016), *Mechanical Vibration–Road Surface Profiles–Reporting of Measured Data*, ISO Geneva, Switzerland (ISO Standard No. ISO 8608:2016(E)).

Ibrahim, I. M., Mokhtar, M. O. A., and El-Butch, A. M. (2003). "New Suspension Design for Heavy Duty Trucks: Design Considerations", *SAE Technical Paper Series 2003-01-3428.*

Kaleemullah, M., Faris, W. F. and FariedHasbullah, N. M. (2019), "Optimization of Robust and LQR Control Parameters for Half Car Model using Genetic Algorithm", *Optimization*, Vol. 28, No. 16, pp. 792-811.

Kuznetsov, A., Mammadov, M., Sultan, I. and Hajilarov, E. (2011), "Optimization of a Quarter-Car Suspension Model Coupled with the Driver Biomechanical Effects", *Journal of Sound and Vibration*, Vol. 330, No. 12, pp. 2937-2946.

Maciejewski, I. (2012), "Design and Optimization of a Control System for Active Vibration Isolators", *Vibrations in Physical Systems*, Vol. 25, pp.273- 278.

Ning, D., Sun, S., Zhang, J., Du, H., Li, W. and Wang, X. (2016), "An Active Seat Suspension Design for Vibration Control of Heavy-Duty Vehicles" *Journal of Low Frequency Noise, Vibration and Active Control*, Vol. 35, No. 4, pp. 264-278.

Paddan, G. S. and Griffin, M. J. (2002) "Evaluation of Whole-Body Vibration in Vehicle", *Journal of Sound and Vibration*, Vol. 253, No. 1, pp.195-213.

Savaresi, S. M., Poussot-Vassal, C. Spelta, C., Sename, O., and Dugard, L. (2010), *Semi-Active Suspension Control Design for Vehicles*, Elsevier Ltd., Oxford, United Kingdom, 206 pp.

Shafie, A. A., Bello, M. M. and Khan, R. M. (2015), "Active Vehicle Suspension Control Using Electrohydraulic Actuator on Rough Road Terrain", *Journal of Advanced Research*, Vol. 9, No. 1, pp.15-30.

Sim, K., Lee, H., Yoon, J. W., Choi, C. and Hwang, S. H. (2017), "Effectiveness Evaluation of Hydro-Pneumatic and Semi-active Cab Suspension for the Improvement of Ride Comfort of Agricultural Tractors", *Journal of Terramechanics*, Vol. 69, pp. 23-32

Song, B. K., An, J. H. and Choi, S. B. (2017), "A New Fuzzy Sliding Mode Controller with a Disturbance Estimator for Robust Vibration Control of a Semi-Active Vehicle Suspension System", *Applied Sciences*, Vol. 7, No. 10, pp.1053.

Su, T. A., Hoe, V. C. W., Masilamani, R. and Awang-Mahmud, A. B. (2011), "Hand-Arm Vibration Syndrome among a Group of Construction Workers in Malaysia", *Occupational Environment Medicine*, Vol. 68, No. 1, pp. 58 – 63.

Tahir, A., Yasin, J., Daneshtalab, M. and Plosila, J. (2014), "Active Suspension System for Heavy Vehicles," *2014 International Symposium on Fundamentals of Electrical Engineering (ISFEE)*, pp. 1-5

Yao, H. J., Fu, J., Yu, M. and Peng, Y. X. (2013), "Semi-Active Control of Seat Suspension with MR Damper" *Journal of physics: conference series*, Vol. 412, No. 1, p. 012054.

Authors

K. Eddah is a PhD candidate at the Mechanical Engineering Department at the University of Mines and Technology (UMaT), Tarkwa, Ghana. He holds a BSc degree in Mechanical Engineering from UMaT and his research interests include Vehicle Dynamics and Fractional-Order Control.

O. A. Dahunsi is a visiting Associate Professor at the Mechanical Engineering Department of the University of Mines and Technology, Tarkwa, Ghana. He holds a PhD degree from the University of the Witwatersrand. He is also a member of the Nigerian Society of Engineers. His present interest is in the application of Mechatronics System Design and Concepts to Manufacturing, Mechanical Vibration, Condition Monitoring and Vehicle Dynamics.

A. Simons is an Associate Professor of Mechanical Engineering Department at the University of Mines and Technology, Tarkwa, Ghana. He holds the degrees of MSc from the Belarusian-Russian University, Magilev, Belarus, PhD from St. Pertersburg State Mining Institute (Technical University) St. Petersburg Russia and NDT Level II from Trinity NDT College Bangalore, India. He is a member of America Society of Mechanical Engineers. and Ghana Institution of Engineering. His research and consultancy works cover Heat Transfer, Fuels and Internal Combusting Engines, Machine Design, Maintenance Engineering, Accident Vehicle Assessment, Factory Technical Audit and Non Destructive Testing (NDT).

S. Nunoo is an Associate Professor at the Department of Electrical and Electronic Engineering, University of Mines and Technology (UMaT). He holds a BSc degree in Electrical Engineering from Western University College of KNUST, now UMaT, Tarkwa, the MPhil degree in Electrical and Electronic Engineering from UMaT, and the PhD in Electrical Engineering at Universiti Teknologi Malaysia, Skudai. He is His research interest is in signal processing for wireless communications with emphasis on adaptive filtering and compressive sampling.